Heritage Science

RESEARCH

Open Access

Chemical, mineralogical and physical study of Late Iron Age ceramics from Nditam: Cameroon (West central Africa)

Epossi Ntah Zoila Luz[1*] and Cultrone Giuseppe[2]

Abstract

This paper studied Late Iron Age ceramic fragments from Nditam village (Centre Region, Cameroon), the technological features and deduced the type of the raw materials used to produce them by combining different analytical techniques based on X-ray fluorescence, powder X-ray diffraction, thermogravimetry, polarized optical microscopy, spectrophotometry and hydric tests. Macroscopic observations suggest the existence of three types of ceramics according to their colour, black, greyish and red, in the two opposite surfaces, outer (or external) and inner (internal). The chemistry indicates that non-calcareous clayey material was used for ceramic production. The correlation between mineralogy, petrography and the geology of the region suggests a local production of ceramics. Moreover, the chemistry of the samples confirms the existence of the three macroscopic groups and suggests the use of local raw materials for their production. From the mineralogical point of view, quartz, feldspar and mica (biotite and muscovite) were identified in all the samples, while kaolinite and amphibole were detected in some of them. The differences in the mineralogy may indicate some variations in the firing temperature, being lower in the ceramics containing kaolinite compared to the other samples. All the samples have similar water absorption behaviour. According to the colours of the ceramics, a prevalence of oxidising firing conditions was present in the kilns. However, partial reducing and short duration firing conditions were also possible. Comparative study with the mineralogy of ethnographic ceramics from southern Cameroon shows some similarities and suggests a continuity in the use of different local clay pits in this region over time.

Keywords Nditam/Cameroon, Ceramics, Petrophysical characterization, Firing technology, Raw material

Introduction and archaeological background

Any ceramic fragment, however insignificant it may appear, can be compared to a "potential book" because it contains as if stored in pages, a wealth of information about its history [1]. Its memory can be activated by a variety of chemical, mineralogical and physical analyses in order to shed light its origin, manufacture, use and burial stage. It should be noted that the technological choices of the potters were always linked to natural resources, the cultural traditions of their community and its natural background. Therefore, the choices of raw materials, ceramic fabrics and recipes, firing conditions and ways of forming vessels are linked to the local environment as much as to the abilities and experience of the potters [2]. In central Cameroon, sixty archaeological sites were discovered during an archaeological excavation in the Tikar area from 1993 to 1997 [3, 4]. These sites were open-air, metallurgical (workshops of iron and bronze production) and rock shelters. The second main excavations in the Tikar area were conducted between

*Correspondence:
Epossi Ntah Zoila Luz
zoila.epossi@univ-yaounde1.cm; zoilaepossi@yahoo.fr
[1] Department of Arts and Archaeology, Faculty of Arts, Letters and Social Sciences, University of Yaounde 1, P.O.Box 755, Yaounde, Cameroon
[2] Department of Mineralogy and Petrology, Faculty of Sciences, University of Granada, Avenida Fuentenueva, s/n18002, Granada, Spain

2005 and 2013 in four sites: Nditam, Ngoumé, Gba and Ngweu [5] (Fig. 1a).

The ceramics selected for the present study come from Nditam (5°00′18″ N and 11°50′31″), a village located in the southern part of the Tikar Area and about 250 km far from of Yaounde in the Centre Region of Cameroon**.** The region is a forest—savannah transition (Fig. 1b).

In Nditam, many pit sites were discovered. Delneuf and Tueche [3] identified a long chronological sequence made up of three main periods. The Nditam phase 1 started from 1319 to 896 BC and was characterized by the presence of the first pit sites, lithic fragments (shards/flakes of quartz) and ceramics with pivoting impression decoration. Nditam phase 2 had two stages, 540–349 BC and 321–206 BC, which were characterized by the beginning of iron metallurgy, the abundance of pits, ceramics with pivoting impressions and lithic materials (stone ball). The Nditam phase 3, the most recent, started from 1487–1603 AD and was characterized by the beginning of the ceramics with roulette decoration patterns and by the continuity of iron metallurgy. The gap between phases 2 and 3 is explained by the absence of data, therefore more excavations and radiocarbon dating are still needed in this region.

Morphological, decorative and stylistic aspects of the ceramics from Nditam have already been studied by Leka [5]. Roulette, comb and fiber impressions were abundant in the most recent ceramics whereas pivoting impressions and incisions were found in the most ancient ones. Morphologically, these ceramics can be classified into flared and narrowed ware characterized by spherical, hemispherical, sub-hemispherical, ellipsoidal, sub-cylindrical and truncated-cone shapes according to the large variety of rim, body and base fragments studied.

A preliminary characterization of the non-plastic inclusions and colour of 5706 ceramic fragments from Nditam was performed by the naked eye and stereomicroscopic observations showing fine to semi-fine pastes with different colours, grey, brown, red and beige [5]. These colours suggest a variety of firing conditions. The non-plastic inclusions were composed of quartz, feldspar, micas, iron nodules, laterite fragments and organic matter imprints. These inclusions were medium to poorly sorted with sizes ranging from 0.5 to 4 mm. Leka [5] suggested the use of a mixture of clays or the addition of sand to the clay to improve the quality of the paste. The study of the provenance of the ceramics was not carried out.

The present paper will centre on selected ceramics belonging to the Nditam phase 3 (1487–1603 AD) to understand the nature of the raw material used in ceramics production and the technology process (clayey material preparation, addition or not of temper and firing conditions) in order to provide those archaeometric data that can help improve and complete the knowledge of ceramic production techniques in Nditam. Although the Nditam area has not yet been examined from the

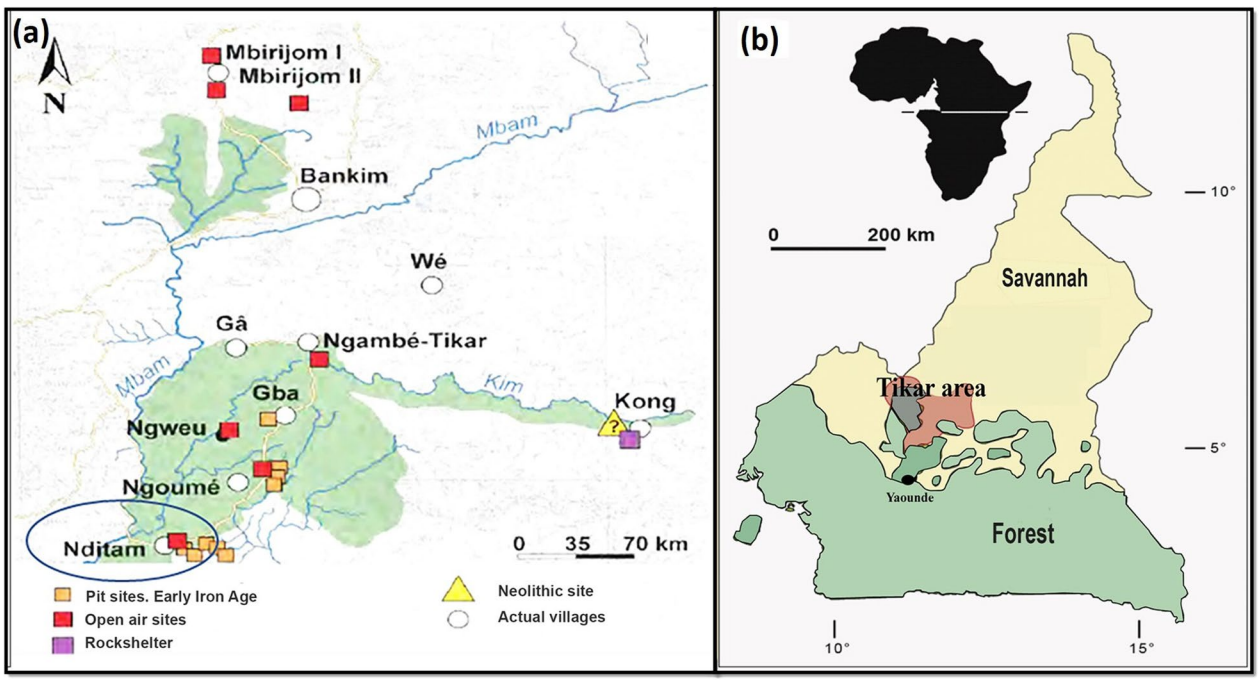

Fig. 1 **a** Archaeological sites found in the Tikar area; **b** location map of the Tikar area in Cameroon from Leka [5]

archaeometric point of view for the study of ceramics, other research has been carried out in the central part of Cameroon, in particular at Mfomakap [6]. Archaeological ceramics from Mfomakap (1905 ± 25 BP) corresponding to the Early Iron Age were characterized by the combined use of chemical, mineralogical and textural techniques with the aim of determining their technology and provenance. For this purpose, local raw materials and ceramic fragments were analysed and compared. In that case, a local production of ceramic products was suggested. In the same line, a mineralogical study of ethnographic ceramics from Bankim, another locality in the Tikar plain was conducted in order to determine the evolution of temperature at different during pre-firing and firing process [7]. The correlation between the analytical techniques suggested that the pre-firing temperature was below 450 °C whereas the firing temperature was between 650–800 °C in a simple bonfire. The present work aims to enhance the contribution of analytical methods in the study of archaeological ceramics from Cameroon as a database for future studies.

In this respect, X-ray Fluorescence will help answer questions about the nature and origin of the raw material used by the potters [8, 9]. X-ray diffraction and thermogravimetric analysis (TG) will be used to identify the mineral phases and inform about the firing temperature whereas the firing atmosphere will be deduced from the macroscopic observations of the ceramics, mainly the colour of the fracture surface [10, 11]. Polarized optical microscopy will be used to analyse the fabric of ceramics to determine the nature of the inclusions present in the paste, clay preparation and nature of temper. Finally, spectrophotometry and hydric tests (water absorption and drying) will complete the characterization of ceramics providing some physical parameter (colour and water flow in the porous system) that will help in defining their quality [12, 13]. These results will give an idea of the technological level of the local potters and to their skills to use natural resources [2].

Geology of the area

The Tikar plain, situated in the Cameroon Central Shear Zone, is part of the North Equatorial Pan-African Belt. It is formed by granitoids rocks intruded sometimes by mafic and intermediate dykes [14]**.** The mafic dykes are essentially banded gabbro with porphyroblastic to porphyritic textures and are composed of plagioclases, pyroxenes, amphiboles, biotite and opaque minerals. The intermediate dykes are monzonites and monzodiorites characterized, respectively, by cataclastic and mylonitic textures [15] and composed of amphiboles, K-feldspar, pyroxenes, epidotes, titanite and opaque minerals. The above-mentioned magmatic rocks are covered in the Tikar plain by clays and sands from the Quaternary age [16]. It is logical to assume that these sediments were used by potters for ceramic production. A schematic geological map of the Tikar plain is presented in Fig. 2.

Materials and methods

Samples

Thirteen ceramic samples of the Late Iron Age (1487–1603 AD) were selected from the collection of the Department of Arts and Archaeology of the University of Yaounde 1 (Cameroon) to be studied in the present paper. All the selected ceramics are shown in Fig. 3**.** They were labelled CNDI 01 to CNDI 13. They show fine to semi fine surfaces and appear macroscopically different on the ornament, colour (external, internal and fracture surface), size and shape. They belong to the rim and body parts of vessels. Except CNDI 08, all the other samples are decorated. The ornaments observed on the surface are simple line bands due to tracing and/or incision (CNDI 01, CNDI 03, CNDI 04 and CNDI 10), impression (CNDI 01, CNDI 02, CNDI 07, CNDI 12 and CNDI 13) and roulette (CNDI 04, CNDI 05, CNDI 09 and CNDI 11).

The thirteen samples were classified in three groups according to their external and internal surface colours:

Group 1 is characterized by a black colour: one sample (CNDI 05).

Group 2 is characterized by a greyish colour (light or dark grey): eight samples (CNDI 03, CNDI 04, CNDI 07, CNDI 08, CNDI 10, CNDI 11, CNDI 12 and CNDI 13).

Group 3 is characterized by a reddish colour (dark or light brown): four samples (CNDI 01, CNDI 02, CNDI 06 and CNDI 09). CNDI 06 and CNDI 01 show some dark areas on their external surface probably due to their use.

Only one sample, CNDI 06, shows a sandwich structure (with a black core), while the rest have brown or reddish fracture surfaces and one sherd, CNDI 04, has a totally dark grey fracture surface. A summary of the main features of the thirteen ceramics is listed in Table 1 and the representative ceramics for the three groups are presented in Fig. 4.

Analytical methods

The chemical composition of ceramics was determined by X-ray Fluorescence (XRF) analysis using a Panalytical Zetium spectrometer equipped with a Rh tube anode and 4 kV X-ray generator. For major elements, a mixture of 0.6 g of powdered sample with 5.4 g of $Li_2B_4O_7$ was melted at 1000 °C; after cooling the disc glass was analysed. For trace elements, a mixture of 5 g of sample in the same proportion with boric acid was pressed to produce a pellet for analyses. The accuracy of the chemical analyses was assessed by comparison with more than 30

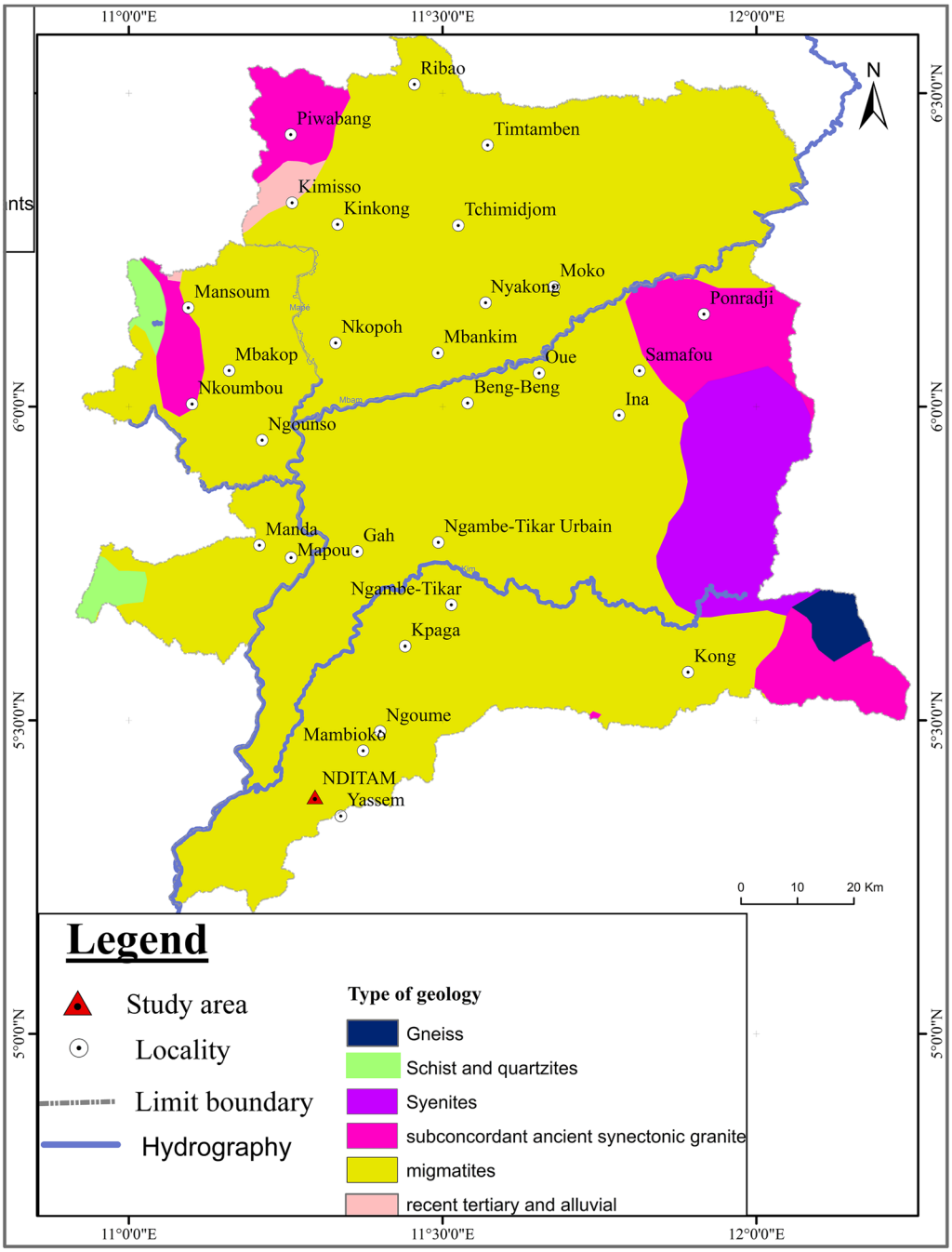

Fig. 2 Schematic geological map of Tikar Plain

certified geostandards covering a wide range of common silicate rocks [17] and XRF intensities were converted to concentrations using the De Jongh model [18]. Typical accuracy is better than 0.1–0.2% relative (0.5% for Na_2O) to a concentration of 10%. Loss on ignition was determined gravimetrically by recording weight loss between 110 ℃ and 1000 ℃. For trace elements, the detection limit is below 1–2 ppm, except for Ba and Co, which are around 10–15 ppm.

Powder X-ray Diffraction (PXRD) analysis was carried out by using a Bruker D8-Advance Eco 1 Kw diffractometer (CuKα radiation, λ = 1.5418 Å, V = 40 kV, I = 25 mA) with a Lynx-eyed X energy-dispersive detector. PXRD patterns were recorded over the 2 -70° (2θ) angular range.

Fig. 3 General view of the thirteen ceramic samples from their external surface (*size of the square edge: 1 cm)*

Table 1 Macroscopic features of the studied ceramic samples

Samples	Group	Ornament	Part of the vessel	Type of ware	Colours		
					External surface	Internal surface	Fracture surface
CNDI 01	3	Impression	Rim	Semi fine	Dark red	Reddish	Reddish
CNDI 02	3	Impression	Body	Semi fine	Dark red	Light brown	Light brown/ reddish
CNDI 03	2	Tracing/ incision	Rim	Fine	Dark greyish	Grey	Reddish
CNDI 04	2	Carved roulette + tracing	Rim	Fine	Light grey	Grey	Dark grey
CNDI 05	1	Carved roulette	Rim	Semi fine	Black	Black	Dark brown
CNDI 06	3	Incision	Rim	Fine	Reddish	Reddish	Sandwich structure with a black core
CNDI 07	2	Impression	Body	Fine	Reddish	Greyish	Light brown
CNDI 08	2	None	Body	Semi fine	Light grey	Light grey	Light brown
CNDI 09	3	Carved roulette	Rim with a lot of mica reflection	Semi fine	Dark red	Dark brown	Reddish
CNDI 10	2	Incision/ tracing	Rim	Fine	Greyish/grey	Light grey	Dark brown
CNDI 11	2	Carved roulette	Rim	Semi fine	Light grey	Light grey	Light brown
CNDI 12	2	Impression	Body	Semi fine	Light grey	Light grey	Light brown
CNDI 13	2	Impression	Body	Fine	Dark brown	Dark grey/	Dark brown

The division into three groups is based on ceramics internal and external surface colours

Fig. 4 Representative ceramics of the three macroscopic groups: **A** external surface; **B** internal surface 1) Group 1: sherd CNDI 05, 2) Group 2: sherd CNDI 08, 3) Group 3: sherd CNDI 01 *(size of the square edge: 1 cm)*

The step size was 0.02° (2θ), whereas the time per step was 48 s. No internal standard was added to the powders. The qualitative identification of mineral phases was carried out using the XPowderX software [19]. According to Garside and Richardson [20], it is important to note that the interpretation of the diffraction pattern is hampered by phase mixing and the technique provides little useful information about the amorphous fraction.

Thermogravimetry (TG) was used to study the thermal reactions of selected ceramics according to their mineralogy to complete the information obtained by PXRD. TG analysis was carried out with a Mettler Toledo TGA/DSC1 apparatus. About 20 mg of sample was deposited on an Al crucible and analysed in a flowing air atmosphere (50 ml/min) at a heating rate of 20 ℃/min in the 25–950 ℃ temperature interval.

For the petrographic study, one thin section per ceramic sample was prepared and observed under a Carl Zeiss Jenapol-U polarized optical microscope (POM). Images in the plane- and crossed-polarized light of the texture and mineralogy were captured with a Nikon D7000 digital camera.

Colour measurements on the surfaces of ceramics were performed with a portable Konica Minolta CM-700d spectrophotometer to determine quantitatively their colour. Lightness (L*) and chromatic coordinates (a* and b*) were determined in the 400–700 nm wavelength range by selecting CIE illuminant D65 that simulates daylight with a colour temperature of 6504 K. Circular areas of the samples with a diameter of 3 mm were analysed (10° vision angle). The illumination was provided by a pulsed xenon lamp with UV cut filter, while a silicon photodiode array detected and measured both incidents and reflected light [21].

Water absorption and drying tests were carried out to assess the hydric behaviour of the ceramics. These tests provide valuable information on the porous system of the materials, predicting their greater or lesser susceptibility to degradation since saline solutions easily circulate through the pores and fissures of materials. The samples used for hydric tests were previously dried in an oven at 70 °C for 24 h to remove any possible moisture.

Free water absorption (A_b), forced (under vacuum) water absorption (A_f), drying index (D_i), degree of pore interconnection (A_x) [22], open porosity (P_o), saturation coefficient (S) and apparent (ρ_b) and real densities (ρ_{sk}) were calculated according to UNE-EN 13755 [23], NORMAL 29/88 [25] and RILEM [24] standards.

Results and discussion

Chemical composition

SiO_2 is the highest compound in all the studied samples. Seven samples (CNDI 05, 06, 07, 08, 10, 11 and 13) exceed 62 wt.%, and the other six are between 53 to 58 wt.% (Table 2). This suggests the presence of quartz and other silicate phases in the studied ceramics. The Al_2O_3 content varies between 16 to 26 wt.% and seems to be related to the presence of phyllosilicates and feldspars *s.l.* [26]. The ratios SiO_2/Al_2O_3 are greater than 2 and indicate the predominance of quartz over clay minerals [27, 28]. These and the following suggestions should be confirmed later, after mineralogical analysis of the samples (Sect. "Powder X-ray diffraction (PXRD) and thermogravimetry (TG)").

The ceramics are all CaO poor, being this compound comprised between 0.3 and 1.9 wt.% (Table 2). Fe_2O_3 is quite high (around 11 wt.%) in three samples (CNDI 01, CNDI 02 and CNDI 09). Six samples (CNDI 03, CNDI 04, CNDI 06, CNDI 10, CNDI 12 and CNDI 13) have the Fe content comprised between 6 to 9 wt.%. The remaining four have Fe content of 3 to 4 wt.%. The high amount of iron content in CNDI 01, CNDI 02 and CNDI 09 justifies the marked red colour of these ceramics observed macroscopically and is maybe due to the presence of hematite [29, 30].

Concerning alkalis, the K_2O content varies between 1.4 to 4 wt.% in all the samples, probably due to the presence of different amounts of K-feldspar and phyllosilicates [31, 32]. Na_2O content is very low and negligible in all the samples.

Table 2 chemical composition of major oxides (in wt.%)

Samples	Group	SiO_2	Al_2O_3	Fe_2O_3	MnO	MgO	CaO	Na_2O	K_2O	TiO_2	P_2O_5	LOI
CNDI 01	3	55.66	20.63	11.27	0.04	2.04	0.79	0.18	1.62	1.54	0.22	5.57
CNDI 02	3	53.21	23.35	11.44	0.08	1.58	0.82	0.56	3.91	2.27	0.21	1.89
CNDI 03	2	57.90	25.47	6.18	0.03	0.88	1.07	0.70	1.38	1.32	0.28	4.09
CNDI 04	2	56.77	25.91	7.29	0.03	1.95	1.83	0.79	1.34	0.79	0.37	2.15
CNDI 05	1	62.11	20.96	3.92	0.03	1.01	0.97	0.59	1.59	0.92	0.88	6.40
CNDI 06	3	63.88	18.39	6.30	0.05	1.25	0.69	0.13	3.36	1.84	0.31	3.11
CNDI 07	2	63.19	24.89	3.08	0.01	0.43	0.83	0.50	2.65	0.77	0.13	2.78
CNDI 08	2	66.25	20.70	3.76	0.03	0.65	0.64	0.15	2.12	2.20	0.19	2.57
CNDI 09	3	57.86	19.89	10.93	0.05	1.95	0.89	0.23	2.54	1.74	0.30	2.93
CNDI 10	2	62.76	19.64	9.10	0.03	1.44	0.78	0.22	1.43	1.30	0.30	2.57
CNDI 11	2	64.49	21.17	3.93	0.03	0.77	0.83	0.69	3.15	1.07	0.21	2.89
CNDI 12	2	58.07	25.41	6.20	0.02	0.68	0.89	0.12	2.82	1.65	0.33	3.02
CNDI 13	2	68.62	15.91	6.06	0.03	1.56	0.4	0.07	2.17	1.02	0.23	3.44

LOI stands for loss on ignition

The percentage of flux oxides ($K_2O + Na_2O + CaO$) in all ceramics is low and consequently they are refractory because the high content of these elements will reduce their melting temperature.

P_2O_5 values are in the range of 0.13—0.37 wt.%, except CNDI 05 sample, which shows content as high as 0.88 wt.%. A value higher than 0.5% generally suggests phosphorus contamination [33]. P_2O_5 could have come from a swamp area or cemetery and, therefore, could have been contaminated by infiltration of water during burial or by daily use [34, 35]. Moreover, CNDI 05 is the sample with the sample with the highest LOI content.

According to the literature, values of LOI over 2% in CaO poor ceramics can be explained by the presence of water absorbed during the burial or by the dehydroxylation of clay minerals still present in ceramics due to firing at low temperatures [36, 37].

Table 3 shows the trace elements (in ppm) of the studied ceramics. The amount of Ba, Cr, Zr and V are high compared to the other measured elements (Table 2). The high Ba content (468 to 1099 ppm) can be explained by the presence of barite crystals or the contamination of the samples during the burial stage [34, 38]. The amount of Cr varies between 138 to 610 ppm and most of the samples do not exceed 280 ppm. The high Cr content in some samples (CNDI 01, CNDI 04, CNDI 10 and CNDI 12) can be explained by the presence of chromite. The amount of Zr varies between 152 and 444 ppm and suggests the existence of zircon. V is in the range 90–278 ppm and may indicate the formation of some vanadate compound.

The variation of the major and trace elements of the studied samples does not appear to be correlated with the macroscopic classification.

Table 3 Chemical composition of trace elements (in ppm)

Samples	Group	Zr	Sc	V	Cr	Co	Ni	Cu	Zn	Ga	Rb	Sr	Y	Nb	Ba	La	Ce	Nd	Sm	Pb	Th
CNDI 01	3	299	32	278	315	16	93	81	113	24	100	75	40	15	900	98	181	82	13	17	12
CNDI 02	3	256	64	227	160	21	80	50	150	28	165	123	50	21	788	85	154	81	15	19	11
CNDI 03	2	336	31	196	222	18	57	73	107	29	73	147	49	16	669	86	156	68	14	21	8
CNDI 04	2	152	29	118	610	24	73	49	109	23	71	151	28	11	1099	33	58	24	7	15	5
CNDI 05	1	295	18	133	161	12	39	26	84	25	113	96	30	11	554	103	189	68	10	19	32
CNDI 06	3	279	26	207	181	15	62	49	90	22	130	77	48	21	662	77	133	71	13	16	7
CNDI 07	2	348	10	90	170	4	53	15	67	34	111	169	19	17	581	67	116	43	9	45	19
CNDI 08	2	373	26	170	138	9	36	39	109	26	150	95	54	22	468	68	100	60	14	18	10
CNDI 09	3	319	36	230	275	16	79	53	115	26	140	83	65	20	737	107	197	98	21	13	15
CNDI 10	2	220	31	182	434	18	96	66	153	23	89	70	22	10	498	46	80	35	8	18	5
CNDI 11	2	444	12	155	247	17	45	22	81	27	138	142	29	20	581	70	135	52	10	28	20
CNDI 12	2	288	27	190	419	16	69	29	80	31	142	172	35	17	887	103	185	59	12	33	9
CNDI 13	2	249	20	156	145	10	41	35	79	17	104	41	28	13	497	40	76	34	8	14	8

Powder X-ray diffraction (PXRD) and thermogravimetry (TG)

The X-ray diffraction patterns show that all the ceramic samples are rich in quartz (Qz) and contain feldspars *s.l.* (Fsp) (Fig. 5) confirming our suggestions based on the results of chemical analysis. Most of samples are also composed of muscovite (Ms), while kaolinite (Kln) and actinolite (Act) were only detected in CNDI 01 and CNDI 04, respectively. The differences in the mineralogy of samples lead to propose the existence of three new groups:

- Mineralogical group 1: quartz + feldspar + kaolinite + muscovite (1 sample);
- Mineralogical group 2: quartz + feldspar + muscovite (10 samples);
- Mineralogical group 3: quartz + feldspar (2 samples).

The differences detected in the three groups may imply changes in the use of raw materials, and/or more likely in the technology production (i.e., addition of temper and firing temperature). As the chemical analysis was unable to differentiate the thirteen samples into distinct groups, it is assumed that only one raw material was used. According to the mineral phases detected by PXRD, the ceramic from group 1 was probably fired below 600 ℃ due to the presence of kaolinite. As this phyllosilicate disappears between 400 and 650 °C [10, 35], its presence in the ceramic means that the firing temperature was not high enough to decompose it. The presence of muscovite in the ceramics (and the absence of kaolinite) from group 2 indicates a firing temperature over 600 °C but below 900 °C because mica disappears around 900–1000 °C [10, 35]. Its presence in the sherds means that their firing temperature was not high enough to decompose it. The third group of samples was fired over 900 °C due to the absence of phyllosilicates [39]. It is curious to note that the hematite is not detected even if the high Fe_2O_3 content determined by XRF. Probably, iron is present in ceramics in an amorphous or poorly crystalline phase.

Based on the mineralogy identified by PXRD, three samples (CNDI 01, CNDI 07 and CNDI 13, i.e., one in each group) were selected to be investigated by thermogravimetry (TG). Figure 6 shows that the three samples present a slight mass loss up to 200 °C, which corresponds to the presence of hygroscopic water [40]. Sample CNDI 01 presents a second weight loss between 400–650 ℃ which is due to the loss of structural water contained in phyllosilicates [10, 40]. In fact, this is the only sample that contains kaolinite (Fig. 5) and the loss is related to the dehydroxylation of this phyllosilicate,

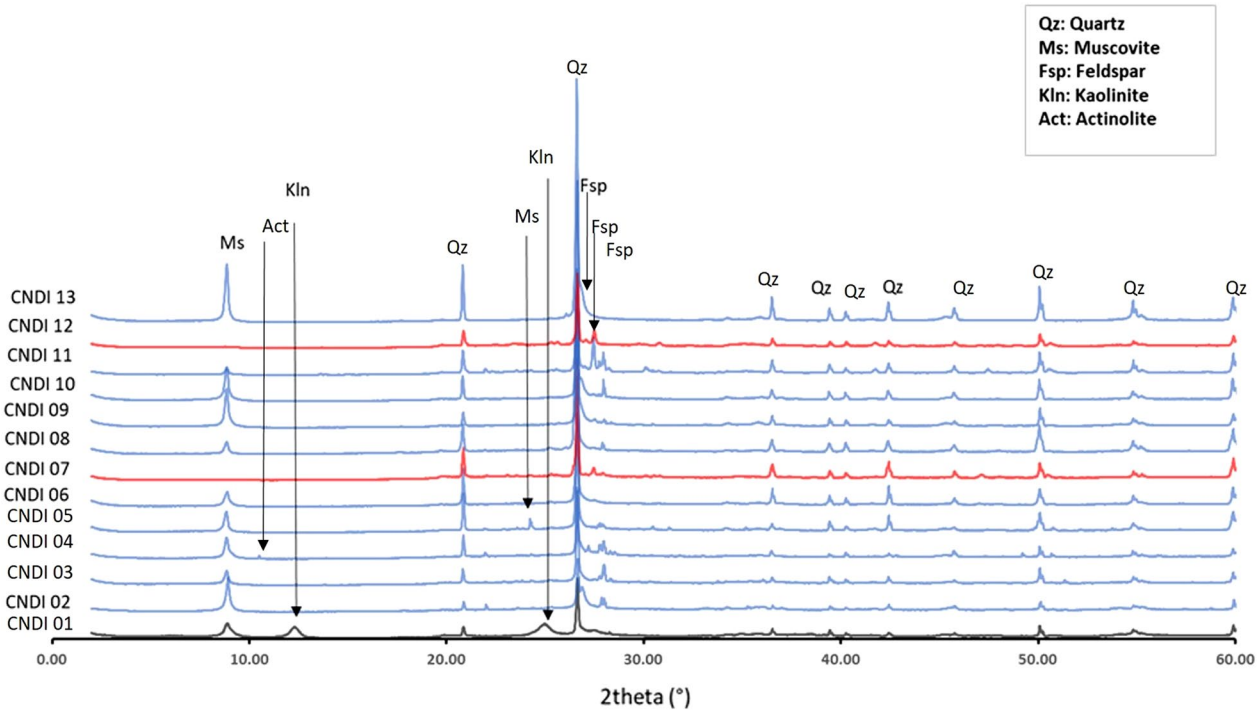

Fig. 5 PXRD patterns of the studied samples. Legend: Ms = muscovite; Kln = kaolinite; Act = actinolite; Qz = quartz; Fsp = feldspar *s.l.* Mineral abbreviations after Warr [42]. Black curve corresponds to the mineralogical Group1, blue curves to mineralogical Group 2 and red curves to mineralogical Group 3

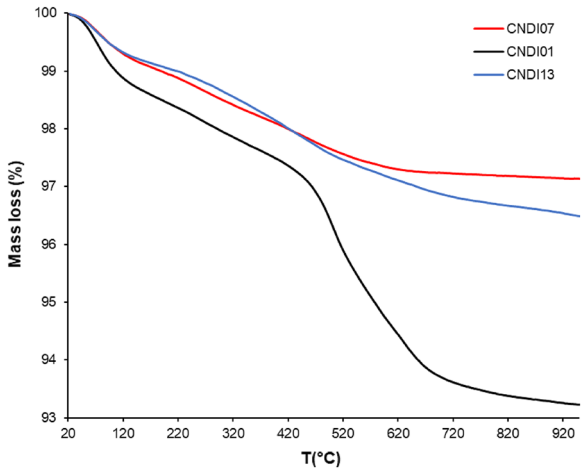

Fig. 6 TG curves of three selected ceramic sherds. Black curve corresponds to CNDI 01 sample that contains kaolinite and muscovite; blue curve corresponds to CNDI 13 sample that contains muscovite; red curve corresponds to CNDI 07 sample that has no clay minerals and therefore is the one that lost the least weight

which turns into metakaolinite according to the following equation:

$$\underset{\text{kaolinite}}{Al_2(OH)_4(Si_2O_5)} \rightarrow \underset{\text{water}}{2H_2O} + \underset{\text{metakaolinite}}{Al_2O_3.2SiO_2}$$

CNDI 01 is the sample that loses the most weight by TG (6.7%) followed by CNDI 13 (3%) and CNDI 07 (2%), whose loss is really low and in agreement with the LOI values obtained by XRF (see Table 2). The slightly higher value of weight loss in CNDI 13 compared to CNDI 07 is attributable to the residual dehydroxylation of the muscovite [41] present in the former, in agreement with PXRD data (Fig. 6). The weight loss of the three samples in the sector with the greatest inflexion of the curves, i.e. between 450–720 ℃, is as follows: CNDI 01 loses 3.5% whereas the lowest weight loss is 0.8% for CNDI 13 and 0.2% for CNDI 07.

Polarized optical microscopy (POM)

Figure 7 shows the main features of the studied ceramics under optical microscopy. The petrographic analysis does not show the same grouping defined after macroscopic observations but agrees with the mineralogy determined by PXRD. All the ceramics are characterized by the presence of quartz, feldspar *s.l.* and phyllosilicates, which constitute the aplastic inclusions, in a matrix that varies from red to black. These aplastic inclusions appear poorly sorted in all the ceramics.

Quartz is the main phase and appears as isolated crystals with undulose extinction and angular morphology or as part of gneiss fragments showing mosaic texture (Fig. 7a). Feldspar *s.l.* is mainly constituted of K-feldspar with often signs of argillification (Fig. 7b) and sometimes cross-hatched twinning. Plagioclase with albite-type twinning is less frequent. Among phyllosilicates, muscovite is prevailing with first-to-second interference order colour, while biotite is sporadic (Fig. 7c). These planar crystals are sometimes oriented due to the pressure exerted to the raw material during moulding (Fig. 7a). Opaque minerals are scattered in the matrix of all samples. The pores are homogeneously distributed in the matrix and are mostly elongated.

Some differences can be detected between samples based on the types or the aplastic inclusions, their abundance, sizes and the presence of accessory minerals. For example, CNDI 04 is the only sample where amphiboles were identified. Based on their colour, these inosilicates have low Fe content, being probably tremolite-actinolite (Fig. 7d). It is also the sample with the highest plagioclase content. Epidote *s.s.* has been observed in CNDI 11 (Fig. 7e), while small zircon crystals were detected in CNDI 01 and CNDI 08 (Fig. 7f). CNDI 06 highlights for the presence of a black core with red rims and a high amount of aplastic inclusions (Fig. 7g). The opposite can be represented by CNDI 01, CNDI 02 and CNDI 12 due to their small grain size. CNDI 12 also shows red levels where small hematite crystals can be distinguished (Fig. 7h). Some differences with the mineralogy identified by PXRD are due to the detection limit of the latter technique or because the crystals sizes are too low to be observed under POM.

Physical analyses: porosity and colour

The studied samples have similar hydric behaviour with absorbed water between 18 and 24% (A_b, Table 4). Only one sample, CNDI 05, is out of this range with a value of 14% (Fig. 8 and Table 4). This difference is maintained when samples undergo forced water absorption (A_f, Table 4).

Regarding the degree of pore interconnection, CNDI 10 is the sample with the poorest pore interconnection (it has the highest A_x value, Table 4) followed by CNDI 13, while CNDI 12, CNDI 09 and CNDI 08 show the best pore interconnection (A_x ranges from 2 to 4) indicating easier water flow in the pore network of these three ceramics. The other samples range between 5 and 9.

The drying of the ceramics (Di, Table 4 and Fig. 8) is very similar in all the samples (values ranging from 0.91 to 0.94), which indicates that they take almost the same time to dry.

Samples that absorbed more water are those that generally attain higher open porosity values (P_o, Table 4). Porosity varies from 32 to 38%, being CNDI 05 the only

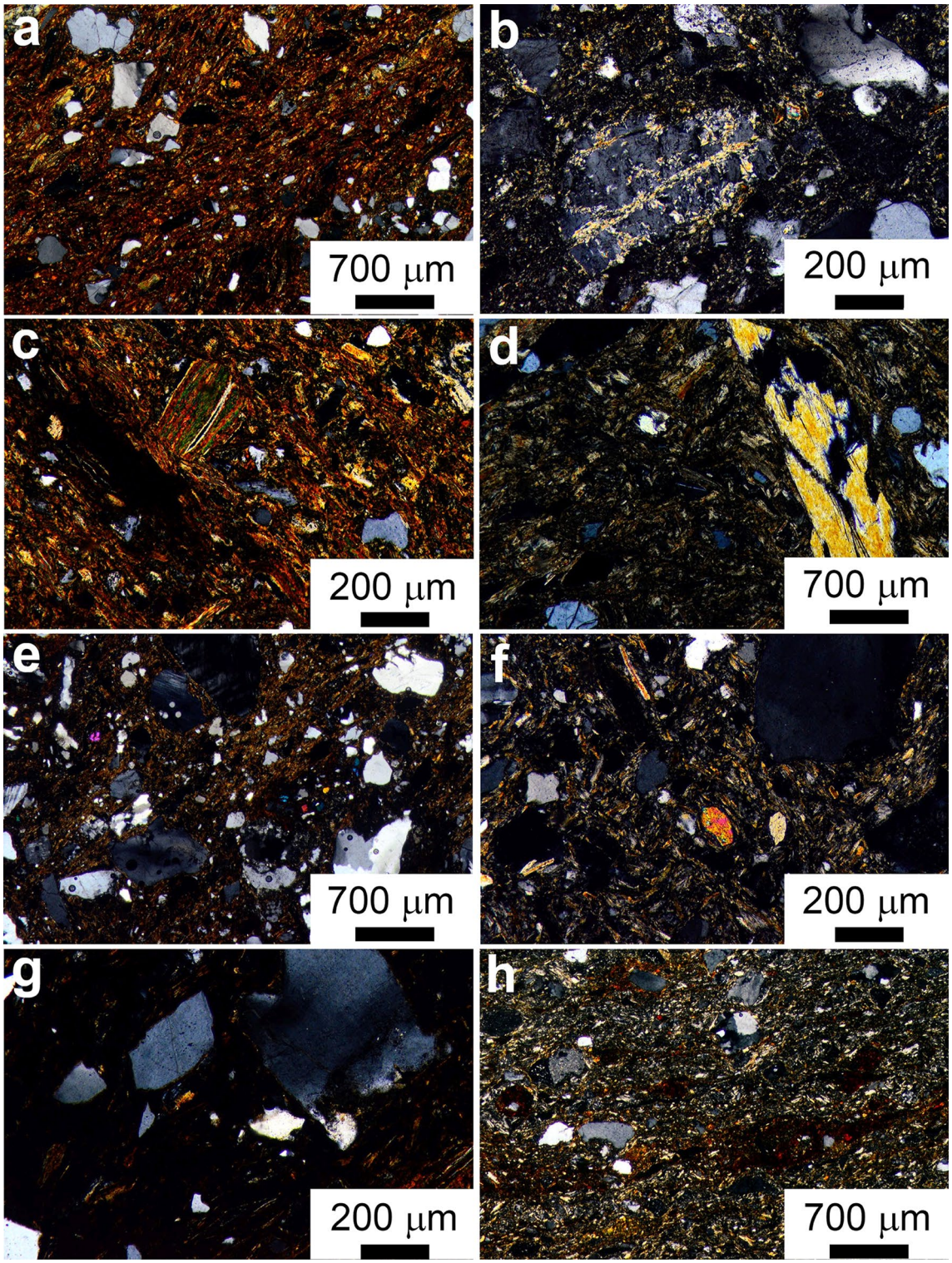

Fig. 7 Polarized optical microscopy (POM) photographs of selected ceramic samples: **a** general view of a reddish matrix in which angular quartz grains grey coloured can be recognized. Note the orientation of phyllosilicates in the matrix; **b** incipient argillification of K-feldspar grain; **c** presence of an isolated biotite grain with speckled extinction; **d** amphibole with first order yellow interference colour observed in the sample CNDI 04; **e** small epidote *s.s.* grains with red to blue interference colours observed in the sample CNDI 11; **f** isolated zircon crystal in CNDI 08 in the centre of the image with high interference colour; **g** presence of quartz grains with angular morphology and undulose extinction in a black core in sample CNDI 06; **h** development of a thin red level composed of Fe oxides in CNDI 12

Table 4 Hydric parameters of the thirteen ceramic samples

Samples	Ab	Af	Ax	Po	Di	ρ_a	ρ_r	S
CNDI 01	24	25	5	38	0.91	1.49	2.40	88
CNDI 02	22	23	5	37	0.92	1.58	2.49	88
CNDI 03	20	21	4	32	0.93	1.58	2.33	88
CNDI 04	20	21	7	33	0.93	1.55	2.31	87
CNDI 05	14	15	9	26	0.94	1.71	2.32	80
CNDI 06	20	22	7	35	0.92	1.62	2.50	89
CNDI 07	18	20	8	33	0.93	1.70	2.55	91
CNDI 08	20	21	4	34	0.93	1.61	2.44	90
CNDI 09	20	21	4	35	0.92	1.66	2.56	91
CNDI 10	18	21	16	34	0.93	1.60	2.43	82
CNDI 11	18	20	9	33	0.93	1.68	2.51	85
CNDI 12	21	22	2	36	0.92	1.62	2.52	95
CNDI 13	19	21	11	36	0.92	1.66	2.58	87

A_b free water absorption (%); A_f forced (under vacuum) water absorption (%); A_x degree of pore interconnection (%); P_o open porosity (%); *Di* drying index; ρ_a apparent density (g cm^{-3}); ρ_r real density (g cm^{-3}); *S* saturation coefficient (%)

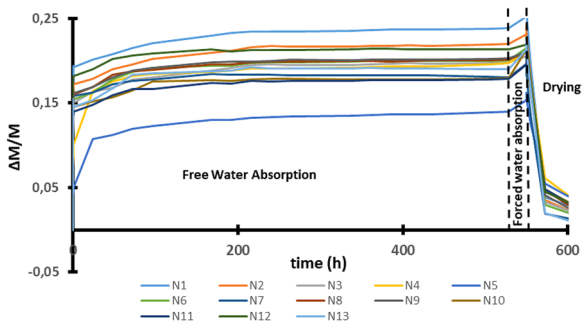

Fig. 8 Free water absorption, forced water absorption and drying curves of the studied ceramic samples. Weight variation (ΔM/M) versus time (in hours). N1 to N13 stand for CNDI 01 to CNDI 13

sample that is out of range with a Po of 26%. In fact, this sample was the one with the lowest water absorption (A_b).

The real density (ρ_r) ranges between 2.3 and 2.6 g/cm^3, values that are typical for ceramic materials and similar to the density of the quartz (2.62 g/cm^3), the main phase identified in the studied ceramics. The values of the apparent density (ρ_a) is clearly lower than ρ_r because it is affected by the amount of empty spaces in the ceramics [43].

The saturation coefficient (S, Table 4) ranges between 80 and 95% and the highest values have been measured in CNDI 09 and CNDI 12 since they were the ceramics with the best pore interconnectivity. According to Cultrone and Madkour [13], S and Ax are inversely related. However, some exceptions are observed, particularly for the sample CNDI 05 which has the lowest saturation coefficient but not the lowest pore interconnection and sample CNDI 10 with the highest Ax value but not the lowest S.

Table 5 Lightness (L*), chromatic coordinates (a*, b*), Chroma (C*) and hue angle (h°) of the ceramic samples using illuminant D65

Samples	L*	a*	b*	C*	h°
CNDI 01	44	6	14	15	66
CNDI 02	45	9	17	19	63
CNDI 03	38	3	7	8	69
CNDI 04	50	6	16	17	68
CNDI 05	33	3	6	7	66
CNDI 06	49	12	21	24	61
CNDI 07	47	8	17	19	65
CNDI 08	54	7	17	18	67
CNDI 09	44	10	18	20	62
CNDI 10	42	7	15	17	67
CNDI 11	39	8	14	16	61
CNDI 12	47	10	19	22	61
CNDI 13	37	6	10	12	60

These exceptions are explained by the loss of small fragments during the development of hydric tests.

Regarding the colorimetry, only two samples attain lightness (L*) higher than 50 (CNDI 08 and CNDI 04) whereas the darker one is measured in CNDI 05 with L* = 33 (Table 5), which is the only black coloured sample. The samples with the highest a* and b* values are CNDI 06 and CNDI 12, those with the most saturated colours (i.e., the highest C* values, Table 5). The least intense colour (lowest a*, b* and C* values) is measured in CNDI 03 and CNDI 05. In the other samples C* varies between 15 and 22. The reflectance curves highlight that samples CNDI 08 and CNDI 06 have high reflectance,

which indicates lighter colours while the lowest has been measured in CNDI 05 (darker colour) (Fig. 9).

Pottery technology and provenance

The study of thirteen ceramics from Nditam by chemical, mineralogical and physical analyses revealed that there is no remarkable difference between the three groups of ceramics distinguished according to macroscopic observations. A non-calcareous raw material was used to produce these ceramics. The high content in quartz with undulose extinction or as a component of gneiss fragments is explained by the presence of metamorphic rocks in the Tikar plain. These rocks supplied quartz and other silicates to the clayey material that was used to make the ceramics [44]. It is important to mention that most of the quartz grains are angular in shape and are not thought to have been added to the paste like sand, which is predominantly rounded. However, some rounded grains are found in the ceramic body, suggesting the presence of sand to improve the quality of the paste by reducing its plasticity.

Moreover, the aplastic inclusions appear poorly sorted in all the samples, indicating that no pre-treatment of the raw material (e.g. crushing and sieving) was done: It seems more likely that the potters used the original clay as collected. The amount of Fe_2O_3 is quite high in several ceramics but this does not correspond to the presence of hematite in PXRD probably due to the presence of poorly crystallized Fe-oxides, even if sporadic hematite crystals have been observed under POM.

The mineralogical composition revealed the presence of quartz, feldspar *s.l.* (mainly K-feldspar and less frequent plagioclase-albite type) and mica (prevalence of muscovite and sporadic biotite) in the ceramics. Kaolinite was detected in the sample (CNDI 01) whereas tremolite-actinolite type amphibole was observed in another (CNDI 04). Kaolinite suggests a very low firing temperature while amphibole is a marker of the geological setting of the region. Due to the identified mineralogy, the firing temperature of the studied samples ranges between 650 and 900 °C except for sample CNDI 01, the one with kaolinite, which was fired below 600 °C. Nevertheless, the presence of the residual kaolinite can also be explained by a thermal cycle, which does not allow a complete transformation of the mineral due to the temperature–time-grain size combination [45]. Further analyses are needed to confirm this suggestion.

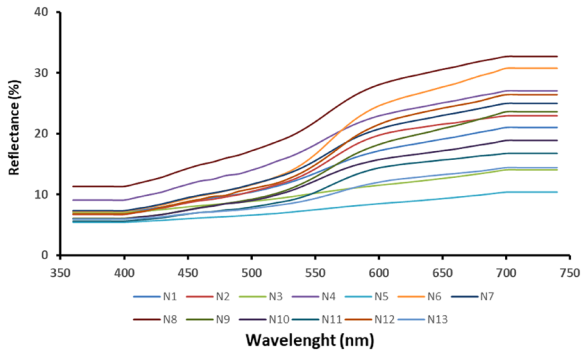

Fig. 9 Reflectance (%) versus wavelength (in nm). N1 to N13 stand for CNDI 01 to CNDI 13

All samples have almost the same hydric behaviour. Only one sample (CNDI 05) is quite different as it absorbs less water and it is the least porous. In general, all the samples have high porosity with the values higher than 19%, which could indicate that they were low fired at around 700 °C according to Daghmehchi et al. [46].

The matrix of most of the ceramics is reddish in brown colour. One sample, CNDI 06, presents a black core with red margins and another sample, CNDI 04, shows a dark grey matrix. The reddish or brown colour of the matrix of the ceramics indicates a firing in an oxidising environment. The samples with black core suggest an incomplete oxidation or most probably a short firing duration whereas the sample with black coloured matrix indicates firing in a reducing environment or the presence of organic matter.

As concerns the provenance of the ceramics, unfortunately, there are no data about the mineralogy and characteristics of the soils in Nditam. This research represents the first compositional studies of a small number of ceramics from this area. However, based on the geological setting of the region and the mineralogical and textural results we have obtained, we suggest a local provenance of the ceramics.

Figure 10 shows scattered plots of SiO_2/Al_2O_3, Fe_2O_3/TIO_2, CaO/MgO and V/Ba. These diagrams highlight that the only sample from the macroscopic Group 1 (CNDI 05) has a similar composition to some ceramics from Group 2. This result suggests that this group of ceramics could have been produced using the same local clay.

The samples from Group 3 show similar composition but some exceptions are observed. In the scatter plots SiO_2/Al_2O_3 and Fe_2O_3/TiO_2, one sample (CNDI 06) of Group 3 is isolated from the others of the same group. This sample shows similarity with those from Group 2. Ceramics from Group 2 are more variable and dispersed in the four diagrams. In addition, sample CNDI 13 is quite isolated in the diagram SiO_2/Al_2O_3 (Fig. 10a) whereas sample CNDI 08 is quite isolated in the diagram Fe_2O_3/TiO_2 (Fig. 10b). The samples CNDI 13 and CNDI 04 are isolated in the scatter plot CaO/MgO (Fig. 10c) whereas the samples CNDI 04 and CNDI 07 are isolated

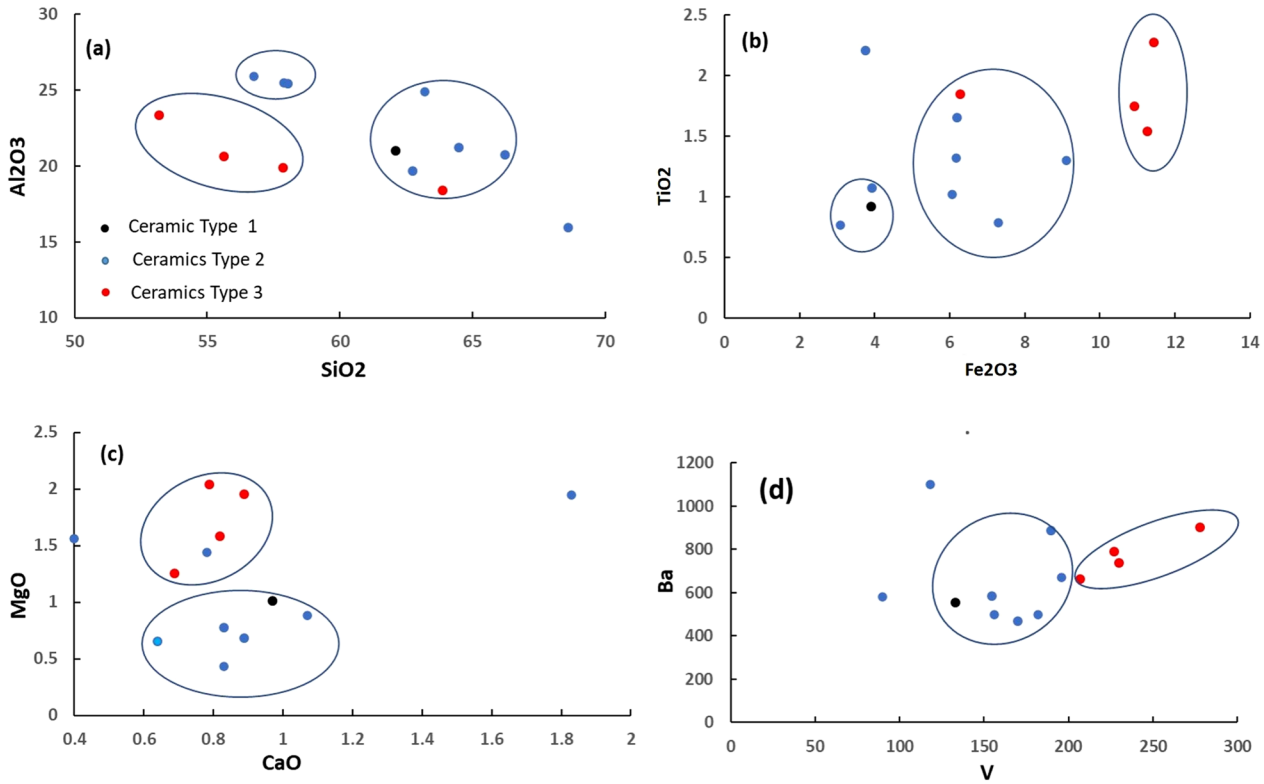

Fig. 10 Chemical correlation diagrams of the ceramic samples **a** SiO_2/Al_2O_3, **b** Fe_2O_3/TiO_2, **c** CaO/MgO in wt.% and **d** V/Ba (this last in ppm). The ceramics are assembled into three groups according to the macroscopic observations described in the Materials and Methods section

in the scatter plot V/Ba (Fig. 10d). The similarities and the diversities observed in the thirteen ceramics suggest some variability in the raw material used to produce them. The chemical variability among the samples underlines the possible use of a variety of raw materials or the sampling of raw materials from the same local clay pit but at different stratigraphic levels.

In the CaO-Na_2O-K_2O ternary diagram (Fig. 11), our ceramics lie between K and Ca, being richer in potassium and very poor in sodium. According to Le Maitre [47] and Nockols and Allen [48], the chemistry of the ceramics studied can be associated with oversaturated acid to saturated intermediate magmatic rocks up to intermediate alkaline rocks, which are not unlike those outcropping in the Tikar plain and supplying the sediments used in the production of Late Iron Age ceramics.

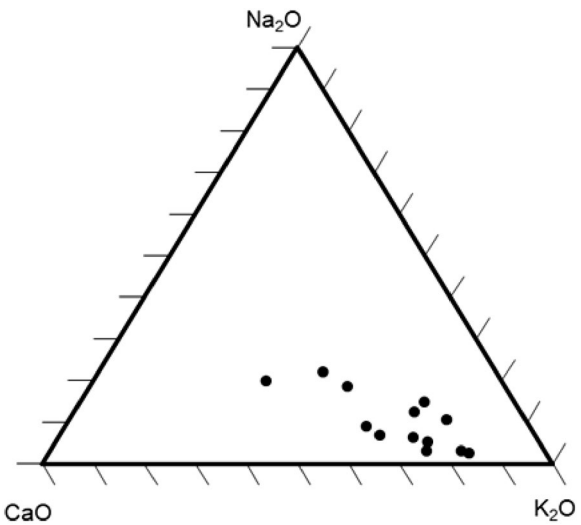

Fig. 11 Ternary diagram Na_2O–K_2O–CaO of the studied ceramics

Comparative studies with southern Cameroon and Ituri forest Congo (RDC) pottery tradition

The studies of Archaeological ceramics or Iron Age ceramics from west Central Africa are mainly focused on their decoration pattern and morphology, the so called "stylistico" morphology approach, to understand the technological distinctions and the pottery tradition over time. The archaeometric approach in this regard is extremely rare. However, in the Democratic Republic of the Congo some archaeometric studies and multi-analytical comparison between Iron Age and ethnographic

ceramics are available Mercader et al. [49] and Tsoupar et al. [50].

Besides this, some ethno-archaeometry studies have been carried out on ceramics from the southern part of Cameroon where the Tikar plain belongs and from some other Africa countries as well (West Central Africa and others countries as Burkina faso, Togo, Nigeria and Niger) by Livingstone Smith [51] and Gosselain [52].

Livingstone smith [51] reported that potters collected raw materials 1- 4 km far from their living area but most of them did it within 1 km (In North Cameroon, Burkina Faso and Togo). These results are in accordance with the work of Mercader et al. [49] who indicated a distance of 1–5 km when studied the late Iron Age and modern ceramics from Ituri Forest of Democratic Republic of the Congo by using an archaeometric approach. The suggestion of local provenance of Iron Age ceramics from Nditam could be correlated with the ethnographic assumptions in Congo and Southern part of Cameroon.

Livingstone Smith [51] distinguished five groups of ethnographic ceramics from southern Cameroon based on petrographic analyses that suggest their provenance from the identification of magmatic rocks and, in some cases, also of metamorphic and sedimentary origin. There is a certain correspondence of our samples with about three of these five groups.

In Ituri Forest (Congo), Mercader et al. [49] reported the existence of very similar mineralogy between raw materials, ancient pottery and modern ceramics. Ituri ceramics were made with clays derived from the local plutonic basement. These clays contain abundant granitic inclusions. Firing took place in bonfires, where shifting oxidising and reducing conditions provided irregularly fired products in the range 600–700 ℃, as suggested by the changes in matrix colour in the same pot and the absence of vitrification in the matrix. This result is in agreement with the estimate of the firing temperature of the ceramics from Nditam at around 800 °C in bonfires. Similar results have been obtained in the mineralogical study of ethnographic ceramics from Bankim a village near Nditam [7] as well as in ethnographic firing systems of ceramics from southern Cameroon [52].

Some small differences are observed in ethnographic and Iron Age ceramics from Cameroon and Congo, mostly on the nature of the temper. Grog and organic matter are used in modern and ancient ceramics from Ituri Forest whereas in the southern part of Cameroon, potters mix different clays and add sand, rock fragments and grog to the paste to improve their workability. The suggestion of sand added to the clayey raw material of Iron Age ceramics from Nditam is deduced from the chemical and petrographic analyses and the archaeological background described by Leka [5]. The similarities in the mineralogy of modern and ancient ceramics lead to the conclusion that pottery production in West Central Africa is a shared tradition in Southern Cameroon and Ituri Forest in Congo.

Similar comparison has been carried out in the composition of archaeological and ethnographic ceramics from Banda in Ghana (West Africa) [53]. The results have shown continuously used clay pits through variably over the course of the second millennium AD.

Conclusions

In this paper, a chemical, mineralogical, textural and physical characterization of thirteen late Iron Age ceramics from Nditam area in the Tikar plain (Centre Region, Cameroon) has been carried out. The macroscopic features of the ceramics based on their colour in the internal and external surfaces enabled us to divide them into three groups: Group 1 (one sample) black, Group 2 (eight samples) greyish and Group 3 (four samples) dark red. Mineralogical, textural and physical analyses do not show remarkable differences among these groups. Quartz, K-feldspars, mica (muscovite and less frequent biotite) and scarce plagioclase were detected in the samples. The presence of kaolinite in one sample indicates a low firing temperature (below 600 °C) whereas the others were fired between 650 and 900 °C. The presence of tremolite-actinolite type amphibole in another ceramic is an indicator of the geological setting of the region where the raw material comes from. Ceramics have almost similar hydric behaviour with some variations regarding their pore interconnection due to the differences in the firing temperature mentioned above. Based on the colour of the ceramics and the presence or not of black cores, the prevalence of oxidising firing conditions is suggested, although reducing and short duration firing conditions are also suggested. The data provided by the mineralogy and petrography suggest a local production of the ceramics. The correlation between chemistry and the macroscopic groups shows that the ceramic from group 1 is close to some ceramics from Group 2, those from Group2 present a variability between them and the ceramics from Group 3 are almost homogeneous except one sample that is close to some ceramics from Group 2. It appears that the studied ceramics were made by using some local raw materials or raw materials from one local clay pit but at different stratigraphic levels. It is logical to assume that the ceramics studied were produced using local clay materials or clays from the same quarry but collected at different points or at different depths, resulting in some compositional variability. Considering the small number of samples studied in this paper, it will be necessary to characterize a larger

number of ceramic fragments and to sample the outcropping clays in the Nditam area to ensure the provenance of the ceramic artifacts. However, this study suggests that the potters from Nditam collected the raw material close to their living area as reported in many ethnographic studies of ceramics from West central Africa. The high quartz content in the ceramics could indicate the addition of sand as temper to improve the workability of the paste. This statement will need to be verified by further studies and would suggests the skill and knowledge acquired by the potters from Nditam. Petrographic comparison of the Iron Age ceramics from Nditam and the ethnographic ceramics in the southern part of Cameroon shows mineralogical similarities over time in some groups of ceramics. This result suggests a continuity in the use of the different local clay pits in this region over time and a shared technological tradition.

Abbreviations

POM	Polarized optical microscopy
XRF	X-ray fluorescence
PXRD	Powder X-ray diffraction
TG	Thermogravimetry
LOI	Loss of ignition

Acknowledgements
We are thankful to the Department of Arts and Archaeology of the University of Yaounde 1 for giving us the samples. We also want to thank the CIM/GIZ (German Cooperation Funds) for their support during the stay in Granada for the analyses. We are also grateful to the Ministry of Higher Education of Cameroon for the research special allowance to lecturers in the cameroonian state universities. Dr. Fabbri Bruno (Institute of Science and Technology for Ceramics -CNR of Faenza/Italy), Dr. Jacques Richard Mache (Mining School of the University of Ngaoundere/Cameroon) and Prof. Mbey Jean Aimé (Faculty of Science of the University of Yaounde1/ Cameroon) deserve our appreciation for their helpful suggestions. Special thanks to Prof. Ubanako Valentine (Bilingual Studies Department of the University of Yaounde 1) for the English proofreading.

Author contributions
EN contributed in the collection of samples, the sampling and analytical works (thin sections, PXRD, XRF, hydric tests, TG, Spectrophotometry) and interpretation of the analytical data as well as preparing the draft of the manuscript and editing. CG contributed in the analytical works (POM, PXRD, XRF, Hydric test, TG) and interpretation of the analytical data as well as preparing and editing the manuscript. Both authors read and approved the final manuscript.

Funding
This study was funded by Junta de Andalucía Research Group RNM179 and the Research Project B-RNM-188-UGR20 of the Regional Ministry of University, Research and Innovation of the Junta de Andalucía and FEDER (Spain), *a way of making Europe*.

Availability of data and materials
The datasets used and/or analysed during the current study are available from the corresponding author on reasonable request.

Declarations

Competing interests
The authors declare that they have non competing interests.

Received: 11 August 2023 Accepted: 16 December 2023
Published online: 02 January 2024

References

1. Maggetti M. Phase analysis and its significance for technology and origin. Olin: JS Franklin, AD Archaeol Ceram Smithson Inst Press; 1982. p. 121–33.
2. Sillar B, Tite MS. The challenge of 'technological choices' for materials science approaches in archaeology. Archaeometry. 2000;42(1):2–20.
3. Delneuf M, Tueche R. Reconnaissance archéologique au sud du pays Tikar. In: ORSTOM, UR 5A. 1994.
4. Elouga M. Recherche archéologique dans la limite forêt-savane: Prospection et inventaire des sites (pays Tikar et Voûté). In: Dynamique à long terme des écosystèmes forestiers intertropicaux. 1996.
5. Leka MJ. Étude des occupations humaines dans la vallée du Mbam: caractérisation des productions céramiques des sites de Ngoume et Nditam au Ier millénaire BC (Cameroun central). Université de Paris 1—Panthéon - Sorbonne; 2013.
6. Epossi Ntah ZL. Archaeometrical studies: petrography, mineralogy and chemistry of selected ceramics sherds and clay samples from Cameroon-Regions of Mombal. Mfomakap and Zamala-: University of Leipzig; 2012.
7. Epossi Ntah ZL, Ossima A, Richard MJ. Ethnographic Ceramics From Bankim (Adamawa, Cameroon / West Central Africa): mineralogical and thermal characterization. Tessituras Rev Antropol e Arqueol. 2022;10(1):132–47.
8. Cultrone G, Molina E, Arizzi A. The combined use of petrographic, chemical and physical techniques to define the technological features of Iberian ceramics from the Canto Tortoso area (Granada, Spain). Ceram Int. 2014;40:10803–16.
9. Borgers B, Ionescu C, Clotuche R, Willems S. Continuity and diversity of Roman pottery production at Famars (northern France) in the 2nd – 4th centuries AD : insights from the pottery waste. Archaeol Anthropol Sci. 2020. https://doi.org/10.1007/s12520-020-01113-2.
10. Epossi Ntah ZL, Sobott R, Fabbri B, Bente K. Characterization of some archaeological ceramics and clay samples from Zamala—Far-northern part of Cameroon (West Central Africa). Cerâmica. 2017;63(367):413–22.
11. Emami M, Vallcorba O, Rozatian ASH, Hadian Dehkordi M, Talaee H, Chapoulie R. Synchrotron micro-XRD applied for the characterization of pottery from the Neolithic to Chalcolithic transitional period: a case study from Tappeh Zaghe, Iran. Eur Phys J Plus. 2021. https://doi.org/10.1140/epjp/s13360-020-01035-x.
12. De Bonis A, Grifa C, Cultrone G, De VP, Langella A, Morra V, Neff H. Raw Materials for Archaeological Pottery from the Campania Region of Italy : A Petrophysical Characterization. Geoarchaeology. 2013;28:478–503.
13. Cultrone G, Madkour F. Evaluation of the effectiveness of treatment products in improving the quality of ceramics used in new and historical buildings. J Cult Herit. 2013;14(4):304–10.
14. Ntieche B, Ram Mohan M, Moundi A, Wokwenmendam NP, Mounjouohou MA, Nchouwet Z, Mfepat D. Petrochemical constrains on the origin and tectonic setting of mafic to intermediate dykes from Tikar plain, Central Cameroon Shear Zone. SN Appl Sci. 2021;3(2):211.
15. Koch P. Sur les mylonites de la plaine Tikar au Sud de Banyo (Cameroun). Bull la Société Géologique Fr. 1953;S6-III(7–8):543–546.
16. Regnoult JM. Synthèse géologique du Cameroun. Yaoundé: Ministère des mines et de l'énergie du Cameroun; 1986. 119 p.
17. Govindaraju K. Compilation of working values and sample description for 383 geostandards. Geostandard Newsletter. 1994;18:1–158.
18. De Jongh WK. X-ray fluorescence analysis applying theoretical matrix corrections. Stainless steel X-ray Spectrom. 1973;2:151–8.
19. Martin JD. XPowder, a software package for powder X-ray diffraction analysis, Lgl. Dep. GR 1001/04. Spain; 2004.
20. Garside P, Richardson E. Analytical methods in conservation. In: Gardise P, Richardson E, editors. Conservation Science: Heritage Materials. Royal Society of Chemistry; 2021. p. 478.
21. Cultrone G, Molina E, Grifa C, Sebastián E. Iberian ceramic production from Basti (Baza, Spain): First geochemical, mineralogical and textural characterization *. Archaeometry. 2011;2(53):340–63.

22. Cultrone G, Sebastian E, Elert K, Jose M, Cazalla O, Rodriguez NC. Influence of mineralogy and firing temperature on the porosity of bricks. J Eur Ceram Soc. 2004;24:547–64.
23. UNE-EN 13755. Métodos de ensayo para piedra natural. Determinación de la absorción de agua a presión atmosférica. AENOR. Madrid; 2008.
24. RILEM. Recommended test to measure the deterioration of stone and to assess the differences of treatment methods. Mater Struct. 1980;13:175–253.
25. NORMAL 29/88. Misura dell'indice di asciugamento (drying index). Rome, ICR-CNR; 1988.
26. Kramar S, Lux J, Mladenović A, Pristacz H, Mirtič B, Sagadin M, Smuč´NR. Mineralogical and geochemical characteristics of Roman pottery from an archaeological site near Mošnje (Slovenia). Appl Clay Sci. 2012;57:39–48.
27. Ndjigui PD, Mbey JA, Fadil-Djenabou S, Onana VL, Bayiga EC, Enock Embom C, Ekosso IG. Characteristics of kaolinitic raw materials from the lokoundje river (Kribi, cameroon) for ceramic applications. Appl Sci. 2021;11(13):6118.
28. Kılıç NÇ, Kılıç S, Akgül HÇ. An archaeometric study of provenance and firing technology of halaf pottery from tilkitepe (Eastern Turkey). Mediterr Archaeol Archaeom. 2017;17(2):35–48.
29. Palanivel R, Kumar UR. Thermal and spectroscopic analysis of ancient potteries. Rom J Phys. 2011;56(1–2):195–208.
30. De Bonis A, Cultrone G, Grifa C, Langella A, Leone AP. Different shades of red : The complexity of mineralogical and physico—chemical factors influencing the colour of ceramics. Ceram Int. 2017;43:8065–74.
31. Daghmehchi M, Rathossi C, Omrani H, Emami M, Rahbar M. Mineralogical and thermal analyses of the Hellenistic ceramics from Laodicea Temple. Iran Appl Clay Sci. 2018;65:146–54.
32. İssi A, Kara A, Alp AO. An investigation of Hellenistic period pottery production technology from Harabebezikan/Turkey. Ceram Int. 2011;37(7):2575–82.
33. Fabbri B, Gualtieri S. Reasons of phosphorus pollution inarchaeological pottery and its consequences: a reassessment. Dev Archaeol Res M Adalslteinn T Olander (eds), Nov Sci Publ New York. 2013;41–66.
34. Maggetti M. Chemical analyses of ancient ceramics : what for? Chimia. 2001;55(No 11):923–30.
35. Bonzon J. Archaeometrical study (petrography, mineralogy and chemistry) of Neolithic ceramics from Arbon Bleiche 3 (Canton of Thurgan, Switzerland). Suisse.: Université de Fribourg; 2005.
36. Fabbri B, Gualtieri S, Shoval S. The presence of calcite in archaeological ceramics. J Eur Ceram Soc. 2014;34:1899–911.
37. Camarda L, Cerchi E, Fabbri B, Gualtieri S, Verardi G. Classification and typology of the pottery from Gotihawa (nepalese Tarai), with particular reference to NBPW. In: Proceedings of the "South Asian Archaeology 2001", Paris,. 2001. p. 35–9.
38. Ruffieux M. la production céramique entre le 9 et le 5 ème siècle avant JC dans le Broye. Cah d' Archeol fribourgeoise. 2005; (N7 Etudes).
39. Cultrone G, Javier F, Rosua C. Applied clay science growth of metastable phases during brick firing : Mineralogical and microtextural changes induced by the composition of the raw material and the presence of additives. Appl Clay Sci. 2020;185: 105419.
40. Meyvel S, Satha P, Velraj G. Thermal characterization of archaeological potsherds recently excavated in Nedunkur, Tamilnadu. India Cerâmica. 2012;58:338–41.
41. Cultrone G. The use of Mount Etna volcanic ash in the production of bricks with good physical-mechanical performance: converting a problematic waste product into a resource for the construction industry. Ceram Int. 2022;48(4):5724–36.
42. Warr LN. IMA–CNMNC approved mineral symbols. Mineral Mag. 2021;85(3):291–320.
43. Oudbashi O, Naseri R, Cultrone G, Egartner I, Arizzi A. The pottery production from the Deh Dumen Bronze age graveyard (South-Western Iran): a chemical, mineralogical and physical study. Herit Sci. 2021;9(1):1–19.
44. Singh P, Sharma S. Journal of archaeological science : reports thermal and spectroscopic characterization of archeological pottery from Ambari. Assam JASREP. 2016;5:557–63.
45. Colomban P. Glasses, ceramics and enamelled objects. In: Garside; P, Richardson E, editors. Conservation Science: Heritage Materials. Royal Society of Chemistry; 2021. p. 478.
46. Daghmehchi M, Coletti C, Hyeok Moon D, Esmaeili Jelodar ME, Omrani H, Reka AA, Nematollahzadeh A, Emami M. Mineralogical and microstructural characterization of ceramics from the fifth and fourth millennium BC in the central plateau of Iran. Open Ceram. 2023;15: 100427.
47. Le Maitre RW. The chemical variability of some common igneous rocks. J Petrol. 1976;17:589–637.
48. Nockolds SR, Allen R. The geochemistry of some igneous rock series. Geochim Cosmochim Acta. 1953;4:105–42.
49. Mercader J, Garcia-Heras M, Gonzalez-Alvarez I. Ceramic tradition in the African forest: characterisation analysis of ancient and modern pottery from Ituri, DR: Congo. J Archaeol Sci. 2000;27:163–82.
50. Tsoupra A, Clist B, da Conceição LM, Moita P, Barrulas P, da Piedade JM, da Silva D, Bostoen K, Mirao J. A multi-analytical characterization of fourteenth to eighteenth century pottery from the Kongo kingdom, Central Africa. Sci Rep. 2022;12(1):1–18.
51. Livingstone SA. Chaîne opératoire de la poterie: références ethnographiques, analyses et reconstitution, vol. 1. Thèse Université Libre de Bruxelles: Musée Royale de l'Afrique Centrale. Université Libre de Bruxelles; 2001.
52. Gosselain OP. Poteries du Cameroun méridional. Styles techniques et rapports á l'identité. Editions C N R S Paris; 2002. 254 p.
53. Stahl AB, das Dores Cruz M, Neff H, Glascock MD, Speakman RJ, Giles B, Smith L. Ceramic production, consumption and exchange in the Banda area, Ghana: Insights from compositional analyses. J Anthropol Archaeol. 2008;27(3):363–81.

Publisher's Note